

## A new DFT method for atoms and molecules in Cartesian grid

Amlan K. Roy\*

Division of Chemical Sciences, Indian Institute of Science Education and Research (IISER),  
Salt Lake, Kolkata-700106, India

### ABSTRACT

Electronic structure calculation of atoms and molecules, in the past few decades has largely been dominated by density functional methods. This is primarily due to the fact that this can account for electron correlation effects in a rigorous, tractable manner keeping the computational cost at a manageable level. With recent advances in methodological development, algorithmic progress as well as computer technology, larger physical, chemical and biological systems are amenable to quantum mechanical calculations than ever before. Here we report the development of a new method for accurate reliable description of atoms, molecules within the Hohenberg-Kohn-Sham density functional theory (DFT). In a Cartesian grid, atom-centered localized basis set, electron density, molecular orbitals, two-body potentials are directly built on the grid. We employ a Fourier convolution method for classical Coulomb potentials by making an Ewald-type decomposition technique in terms of short- and long-range interactions. One-body matrix elements are obtained from standard recursion algorithms while two-body counterparts are done by direct numerical integration. A systematic analysis of our results obtained on various properties, such as component energy, total energy, ionization energy, potential energy curve, atomization energy, etc., clearly demonstrates that the method is capable of producing quite accurate and competitive (with those from other methods in the literature) results. In brief, a new variational DFT

method is presented for atoms and molecules, *completely* in Cartesian grid.

**KEYWORDS:** DFT, many-electron systems, Cartesian grid, xc functional

### I. INTRODUCTION

Calculation of wave functions of large molecules by *first principles* methods has been an outstanding problem having much relevance in varied fields such as theoretical chemistry, condensed matter physics, material science, etc. On the one hand, there are standard Roothaan-Hartree-Fock (RHF)-type methods, as implemented in several quantum chemistry program packages, though not difficult are certainly tedious and cumbersome indeed, if the number of basis functions becomes large (which is easily the case for even reasonably smaller molecules). Also these methods ignore the important effects arising from electron correlation. On the other side, there are numerous semi-empirical methods, which admittedly have often found various successful applications in describing molecular properties, but raises many questions regarding their applicability for some systems such as transition metal complexes with different kind of ligands. They suffer from the well-known problem of parametrization; stated differently, a certain parametrization scheme is usually successful for a restricted class of compounds with respect to a restricted number of properties.

Over the last three decades, there has been considerable progress in the formulation and implementation of density functional methods, of

---

\*akroy@chem.ucla.edu, akroy@iiserkol.ac.in

which  $X\alpha$  or Hartree-Fock-Slater, is the simplest, best known. The primary reason for this is because it can account for electron correlation effects in a rigorous, quantitative, transparent manner. Moreover it also provides a good compromise between computational cost and accuracy. Some other popular routes toward introducing electron correlation in a many-electron problem are through Moller-Plesset (MPn) and coupled cluster methods. Density functional theory (DFT) [1–15], in particular, has become a powerful and versatile tool in recent years; and more preferable to the other correlated methods, partly because of its favorable scaling (which is typically  $N^3$ , although recently linear-scaling methods have been available). Obviously, the ultimate goal is to be able to describe structure, dynamics, properties of larger and larger systems as accurately as possible (close to experimental results) with optimal computational resources. Recent dramatic explosion in computer technology and emergence of accurate density functional techniques, in both formalism and algorithmic aspects, have made it possible to reach this goal which has eluded quantum chemistry for long. In more practical terms, this is achieved through a successful marriage of basis-set approaches to electronic structure theory and efficient grid-based quadrature schemes to produce a scaling which is at least as good as self-consistent methods. This also simultaneously allows the very difficult many-body effects to be approximated by an effective *one-electron* potential. A proliferation of DFT-based methodologies has been witnessed for electronic structure calculation of a broad range of systems including atoms, molecules, clusters, solids and this continues to grow at a rapid pace.

The key concept of DFT is that all desired properties of a many-electron interacting system can be obtained in terms of the ground-state electron density,  $\rho(\mathbf{r})$ , in stead of a complicated many-electron wave function, as in traditional *ab initio* approaches. This real, non-negative, 3D, scalar function of position is easily visualizable (in contrast to the wave function which is, in general, complex,  $4N$  dimensional and not so easily interpretable visually). It has *direct* physical significance (can be directly measured experimentally) and, in principle, provides all the informations about *ground and all excited states*,

as obtainable from a wave function. Initial attempts to use electron density as a basic variable for a many-electron system, is almost as old as quantum mechanics and is due, independently to, Thomas and Fermi [16, 17]. In this quantum statistical model, kinetic energy of an interacting system is approximated as an explicit functional of density (by assuming electrons to be in the background of a non-interacting homogeneous electron gas), while electron-nuclear attraction and electron repulsion contributions are treated classically. However, since this completely ignores the important exchange, correlation effects and kinetic energy is approximated very crudely, results obtained from this method are rather too crude to be of any use. It also fails to explain the essential physics and chemistry such as shell structure of atoms and molecular binding. Significant improvements were made by Dirac [18] by introducing exchange effects into the picture, the so-called local density approximation (LDA).

The stark simplicity of these above procedures encouraged multitude of solid-state and molecular calculations. However, due to a lack of rigorous foundation as well as considerably large errors encountered in these works, the theory lost its charm and appeal until a breakthrough work by Hohenberg and Kohn [19], which rekindled the hope. This changed the status of DFT as it got a firm footing and laid the groundwork of all of today's DFT. The first theorem simply states that the external potential  $v_{\text{ext}}(\mathbf{r})$ , and hence total energy of an interacting system is a unique functional of  $\rho(\mathbf{r})$ . According to the second theorem, ground-state energy can be obtained variationally, i.e., the density that minimizes total energy is the exact ground-state density. Note that although these theorems are very powerful, they merely prove the *existence* of a functional, but do not offer any route of computing this density in practical terms. Even though a mapping between ground-state density and energy is established, it remains mute about the construction of this "universal" functional. Thus as far as computational DFT is concerned very little progress is made compared to the prevailing situation. One still needs to solve the many-body problem in presence of  $v_{\text{ext}}(\mathbf{r})$ .

The situation changed dramatically in the following year after the publication of a seminal work by

Kohn and Sham [20], who proposed a clever route to approach the unknown universal functional. This is done by mapping the full interacting system of interest with the real potential onto a fictitious, non-interacting system of particles. The electrons move in an effective Kohn-Sham (KS) single-particle potential  $v_{KS}(\mathbf{r})$  and the auxiliary system yields same ground-state density as the real interacting system, but greatly simplifies our calculation. Since exact wave functions of non-interacting fermions are represented by Slater determinants, major portion of kinetic energy can be computed to a good accuracy, in terms of one-electron orbitals which construct the reference system. The residual unknown contribution of kinetic energy (which is a fairly small quantity) is dumped in to the unknown, non-classical component of electron-electron repulsion as,

$$\begin{aligned} F[\rho] &= T_s[\rho] + J[\rho] + E_{xc}[\rho] \\ E_{xc}[\rho] &= (T[\rho] - T_s[\rho]) + (E_{ee}[\rho] - J[\rho]) = T_c[\rho] + E_{nc}[\rho]. \end{aligned} \quad (1)$$

$T_s[\rho]$  signifies exact kinetic energy of the hypothetical non-interacting system;  $J[\rho]$  the classical component of electron-electron repulsion. In this partitioning scheme then,  $E_{xc}[\rho]$  contains everything that is unknown, i.e., non-classical electrostatic effects of electron-electron repulsion as well as the difference between true kinetic energy  $T_c[\rho]$  and  $T_s[\rho]$ . Now one can write the single-particle KS equation in standard form,

$$\left[ -\frac{1}{2}\nabla^2 + v_{eff}(\mathbf{r}) \right] \psi_i(\mathbf{r}) = \varepsilon_i \psi_i(\mathbf{r}) \quad (2)$$

with the ‘‘effective’’ potential  $v_{eff}(\mathbf{r})$  including following terms,

$$v_{eff}(\mathbf{r}) = v_{ext}(\mathbf{r}) + \int \frac{\rho(\mathbf{r}')}{|\mathbf{r} - \mathbf{r}'|} d\mathbf{r}' + v_{xc}(\mathbf{r}) \quad (3)$$

where  $v_{eff}(\mathbf{r})$  and  $v_{ext}(\mathbf{r})$  signify the effective and external potentials respectively. Exact form of exchange-correlation (XC) functional remains unknown as yet and its accurate form is necessary for description of real interacting systems (such as binding properties). Numerous approximations have been suggested for this and development of improved functionals has constituted one of the most fertile areas of research for several years and even today.

For practical purposes, minimization of the explicit functional is not an easy or efficient task; and hence not recommended. A far more attractive route is, in stead of working *solely* in terms of density, one might bring back the usual orbital picture in to the problem. This gives an appearance like a single-particle theory, albeit incorporating the many-body effects, in principle, *exactly*. In straightforward *real-space* [21–33] solution of this equation, the wave functions are sampled on a real grid through either of the following three representations such as finite difference (FD), finite element (FE) or wavelets where the solution is obtained in an iterative mechanism. The advantage is that, in all cases, relevant discrete differential equations offer highly structured, banded sparse matrices. Moreover, the potential operator is diagonal in coordinate space; Laplacian operator is nearly local (making them ideal candidates for linear-scaling approaches), and these are easily amenable to domain-decomposition parallel implementation. One can use adaptive mesh refinements or coordinate transformations to gain further resolution in local regions of space. The *whole* molecular grid belongs to either uniform [30, 34, 35] or refined uniform grids [23–26, 29, 32, 33]. The classical electrostatic potential can be found using highly optimized FFTs or real-space multigrid algorithms. Using FD and FE approach, reasonably successful, fully numerically converged solution for self-consistent KS eigenvalue problem of atoms/molecules has been reported in literature [21–23]. In another development, an atom-centered numerical grid [22] was proposed for performing molecular-orbital (MO) calculation. The physical domain was partitioned into a collection of single-center components with radial grids centered at each nucleus. Later, a high-order real-space pseudo-potential method [34, 35] was presented for relatively larger systems in uniform Cartesian coordinates. In an orthogonal 3D mesh, an  $m^{\text{th}}$  order FD expansion of the Laplacian can be written as,

$$\left[ \frac{\partial^2 \psi}{\partial x^2} \right]_{x_i, y_j, z_k} = \sum_{-m}^m C_m \psi(x_i + mh, y_j, z_k) + O(h^{2m+2}) \quad (4)$$

The Hartree potential is obtained by a direct summation on grid by an iterative summation technique. FD method has been used in different

flavors [27, 28, 31, 34, 35] for a number of interesting *ab initio* self-consistent problems in clusters and other finite systems, such as forces, molecular dynamics simulations, polarizabilities of semiconductor clusters as well for areas outside traditional electronic structures. Multigrid methods [32, 36, 37], which accelerate the self-consistent procedure by reducing number of grid points considerably, have found many applications in calculations for molecules and large condensed phase systems on uniform grids. Use of these in conjunction with adaptive grid to enhance the resolution [27, 38] has been studied. Convergence is influenced by parameters like grid spacing, domain size, order of representation, etc.

Some of the shortcomings of above approaches are that these are non-variational and dimension of the Hamiltonian matrix is unmanageably large. In an alternative approach, finite expansion bases of localized one-electron functions is employed, such as exponential functions (STO), Gaussian type orbitals (GTO), plane waves (PW), wavelets, numerical basis sets, linear muffin-tin orbitals, delta functions or some suitable combinations of these. With STOs or other numerical orbitals, relevant multicenter integrals in the Hamiltonian needs to be evaluated numerically, while with a Gaussian basis, these and all other integrals required to compute the matrix elements of Hamiltonian, can be obtained analytically. One pays a price for using the latter; for considerably larger number of such functions are required for accurate description of electronic states, as they do not exhibit correct behavior at either small or large distances from nuclei. Gaussian bases have been extensively used in quantum chemistry calculations of small and medium molecules, whereas PWs (frequently coupled with pseudopotentials to treat core electrons) have been most successful for solids. PWs share with Gaussians the same property that the integrals are known analytically. However, unlike Gaussians, Coulomb interaction is local in Fourier space--hence solving Poisson's equation, a very important step in any DFT calculation, is quite trivial in a PW basis. The two notable

disadvantages of PW bases are: (i) periodic boundary conditions must be used, which is desirable for solids, but not so in case of clusters or molecules (ii) resolution of the basis is exactly same everywhere. Thus for atoms and molecules Gaussian bases have been most successful and popular. Combination of GTO and PW bases have also been used [39, 40], whereby KS MOs are expanded in Gaussian bases and the electron density in an augmented PW basis.

Most of the modern DFT programs, for routine calculations, typically employ the so-called atom-centered grid (ACG), pioneered by Becke [41], where a molecular grid is efficiently described in terms of some suitable 3D numerical quadratures. This is not necessarily the best strategy, but is a relatively simpler well-defined path, adopted by majority of DFT programs. The basic step consists of partitioning a molecular integral into single-center discrete overlapping atomic components. For an arbitrary integrand  $F(\mathbf{r})$ , such a decomposition provides the value of integral  $I$  as,

$$I = \int F(\mathbf{r}) d\mathbf{r} = \sum_A^M I_A, \quad \text{for } M \text{ nuclei} \quad (5)$$

such that the atomic integrand  $F_A$ , when summed over all nuclei, returns our original function. Single-center atomic contributions are denoted by  $I_A = \int F_A(\mathbf{r}) d\mathbf{r}$

$$\sum_A^M F_A(\mathbf{r}) = F(\mathbf{r}) \quad (6)$$

$F_A(\mathbf{r})$ s are typically constructed from original integrand by some well-behaved weight functions  $F_A(\mathbf{r}) = w_A F(\mathbf{r})$ . The atomic grid constitutes of a tensor product between radial part defined in terms of some quadrature formulas such as Gauss-Chebyshev, Gaussian, Euler-McLaurin, multi-exponential numerical, etc., [42–49] and Lebedev angular quadratures (order as high as 131 has been reported, although usually much lower orders suffice; 59<sup>th</sup> order being the one most frequently used) [50–54]. Once  $F_A$ s are determined,  $I_A$ s are computed on grid as follows (in polar coordinates),

$$I_A = \int_0^\infty \int_0^\pi \int_0^{2\pi} F_A(r, \theta, \phi) r^2 \sin\theta dr d\theta d\phi \approx \sum_p^P w_p^{rad} \sum_q^Q w_q^{ang} F_A(r_p, \theta_q, \phi_q), \quad (7)$$

where  $w_p^{\text{rad}}$ ,  $w_q^{\text{ang}}$  signify radial, angular weights respectively with P,Q points (total number of points being P×Q). Usually angular part is not further split into separate  $\theta$ ,  $\phi$  contributions as surface integrations on a sphere can be done numerically quite easily accurately by the help of available highly efficient algorithms. Also angular integration has been found to be much improved by Lobatto scheme [44]. Many variants of this integration scheme have been proposed thereafter, mainly to prune away any extraneous grid points, which is much desirable and useful. Integration by dividing whole space and invoking product Gauss rule [55] has been suggested as well. A variational integration scheme [56] divides molecular space into three different regions such as atomic spheres, excluded cubic region and interstitial parallelepiped. In a Fourier transform Coulomb and multi-resolution technique, both Cartesian coordinate grid (CCG) and ACG were used [57–59]; former divides Gaussian shell pairs into “smooth” and “sharp” categories on the basis of exponents while latter connects these two by means of a divided-difference polynomial interpolation to translate density and gradients from latter to former. Among other methods, a partitioning scheme [60], linear scaling [61] and adaptive integration schemes [46, 60, 62] are worth mentioning.

The purpose of this article is to present an alternate DFT method for atoms and molecules by using a linear combination of GTO expansion for the KS molecular orbitals within CCG *solely* [63–65], that has been developed by this author during the past three years. No auxiliary basis set is invoked for charge density. Quantities such as localized atom-centered basis functions, MOs, electron density as well as classical Hartree and non-classical XC potentials are constructed on the 3D real grid directly. A Fourier convolution method, involving a combination of FFT and inverse FFT [66, 67] is used to obtain the Coulomb potential quite accurately and efficiently. Analytical one-electron Hay-Wadt-type effective core potentials [68, 69], which are made of sum of Gaussian type functions, are used to represent the inner core electrons whereas energy-optimized truncated Gaussian bases are used for valence electrons. The validity and performance of our method is

demonstrated in detail for a modest number of atoms and molecules by presenting total energy, energy components, orbital energy, potential energy curve, atomization energy for both local [70] and non-local Becke exchange [71]+Lee-Yang-Parr (LYP) [72] correlation energy functionals. Success of these above mentioned functionals for various physical, chemical processes are well known. However, in absence of the exact functional form although these provide very good estimates, in many occasions they behave rather poorly. Thus construction of more accurate elaborate sophisticated XC functional lies at the forefront of current research activity as evidenced by an enormous amount of literature on this. Some frequently used functionals in recent years are generalized gradient expansion, hybrid, meta or orbital-dependent functionals, etc. (see, for example, [73], for a brief review). In order to expand the scope, applicability and feasibility of our method, we have employed two other relatively lesser used functionals holding good promise, viz., Filatov-Thiel (termed as FT97 in the community) [74, 75] and PBE [76] functionals, which have been used in many applications with quite decent success. Detailed comparisons are made with the widely used GAMESS quantum chemistry program [77] (grid-based method in ACG and gridless method), and wherever possible, with experimental results as well. While this work exclusively deals with pseudopotential studies, full calculations may be investigated in future communications. The article is organized as follows. Section II gives a brief summary of the methodology. A discussion on our results is presented in Section IV, while we end with a few concluding remarks in Section V.

## II. METHODOLOGY AND COMPUTATIONAL CONSIDERATIONS

Details of this method has been published elsewhere [63–65]; here we summarize only the essential steps. Our starting point is the single-point KS equation for a many-electron system, which, under the influence of pseudopotentials, can be written as (henceforth atomic units employed unless otherwise mentioned),

$$\left[ -\frac{1}{2}\nabla^2 + v_{\text{ion}}^p(\mathbf{r}) + v_H[\rho](\mathbf{r}) + v_{\text{xc}}[\rho](\mathbf{r}) \right] \psi_i(\mathbf{r}) = \varepsilon_i \psi_i(\mathbf{r}). \quad (8)$$

Here  $V_{ion}^P$  denotes the ionic pseudo-potential for the system as,

$$V_{ion}^P(\mathbf{r}) = \sum_{R_a} V_{ion,a}^P(\mathbf{r} - \mathbf{R}_a) \quad (9)$$

with  $V_{ion,a}^P$  signifying the ion-core pseudopotential associated with an atom A, situated at  $\mathbf{R}_a$ .  $v_H[\rho(\mathbf{r})]$  describes the classical Hartree electrostatic interactions among valence electrons, while  $v_{xc}[\rho(\mathbf{r})]$  represents the non-classical XC part of the Hamiltonian, which normally depends on electron density (and also probably gradient and other derivatives), but not on wave functions explicitly.  $\{\psi_i^\sigma(\mathbf{r})\}$ ,  $\sigma = \alpha$  or  $\beta$ , corresponds to the set of N occupied orthonormal MOs, to be determined from the solution of this equation.

As already hinted, the so-called, linear combination of atomic orbitals (LCAO) ansatz is by far, the most popular, convenient and practical route towards an iterative solution of molecular KS equation. In this scheme, the unknown

KS MOs  $\{\psi_i^\sigma(\mathbf{r})\}$ ,  $\sigma = \alpha, \beta$  are linearly expanded in terms of a set of K known basis functions as,

$$\psi_i^\sigma(\mathbf{r}) = \sum_{\mu=1}^K C_{\mu i}^\sigma \chi_\mu(\mathbf{r}), \quad i=1,2,\dots,K, \quad (10)$$

where set  $\{\chi_\mu(\mathbf{r})\}$  denotes the contracted Gaussian functions centered on constituent atoms while  $\{C_{\mu i}^\sigma\}$  contains contraction coefficients for the orbital  $\psi_i^\sigma(\mathbf{r})$ . The above expression is exact for a complete set  $\{\chi_\mu\}$  with  $K=\infty$  and, in principle, any complete set could be chosen. However for practical purposes, infinite basis set is not feasible and one is restricted to a finite set; thus it is of utmost importance to choose suitable basis functions such that the approximate expansion reproduces unknown KS MOs as accurately as possible. The procedure is very similar to that applied in HF theory and more practical details could be found in the elegant books [78–80]. Individual spin-densities are then given by,

$$\rho^\sigma(\mathbf{r}) = \sum_i^{N^\sigma} \sum_{\mu=1}^K \sum_{\nu=1}^K C_{\mu i}^\sigma C_{\nu i}^\sigma \chi_\mu(\mathbf{r}) \chi_\nu^*(\mathbf{r}) = \sum_{\mu} \sum_{\nu} P_{\mu\nu}^\sigma \chi_\mu(\mathbf{r}) \chi_\nu^*(\mathbf{r}), \quad (11)$$

where  $P^\sigma$  stands for the respective density matrices. Denoting the one-electron KS operator in parentheses of Eq. (5) by  $f^{KS}$ , one can write the KS equation in following operator form,

$$f^{KS} \psi_i(\mathbf{r}) = \epsilon_i \psi_i(\mathbf{r}). \quad (12)$$

This operator differs from another similar Fock operator  $f^{HF}$  used in HF theory, in the sense that former includes all non-classical many-body effects arising from electron-electron interaction through XC term (as a functional derivative with respect to density,  $v_{xc}[\rho] = \delta E_{xc}[\rho]/\delta\rho$ ), whereas there is no provision for such effects in the latter. This represents a fairly complicated system of coupled integro-differential equation whose numerical solution is far more demanding and some details are mentioned in the following.

In a spin-unrestricted formalism, substitution of energy terms in to the energy expression, followed by a minimization with respect to unknown coefficients  $C_{\mu i}^\sigma$  with  $\rho(\mathbf{r}) = \rho^\alpha(\mathbf{r}) + \rho^\beta(\mathbf{r})$  and  $P = P^\alpha + P^\beta$ , leads to the following matrix KS equation, which is reminiscent of Pople-Nesbet equation in HF theory,

$$F^\alpha C^\alpha = S C^\alpha \epsilon^\alpha, \quad \text{and} \quad F^\beta C^\beta = S C^\beta \epsilon^\beta, \quad (13)$$

with the orthonormality conditions,

$$(C^\alpha)^\dagger S C^\alpha = 1, \quad \text{and} \quad (C^\beta)^\dagger S C^\beta = 1. \quad (14)$$

Here  $C^\alpha, C^\beta$  are matrices containing MO coefficients, S is the atomic overlap matrix, and  $\epsilon^\alpha, \epsilon^\beta$  are diagonal matrices of orbital eigenvalues.  $F^\alpha, F^\beta$  are KS matrices corresponding to  $\alpha, \beta$  spins respectively, having matrix elements as,

$$F_{\mu\nu}^{\alpha} = \frac{\partial E_{KS}}{\partial P_{\mu\nu}^{\alpha}} = H_{\mu\nu}^{\text{core}} + J_{\mu\nu} + E_{\mu\nu}^{XC\alpha}, \quad \text{and}$$

$$F_{\mu\nu}^{\beta} = \frac{\partial E_{KS}}{\partial P_{\mu\nu}^{\beta}} = H_{\mu\nu}^{\text{core}} + J_{\mu\nu} + E_{\mu\nu}^{XC\beta}. \quad (15)$$

Here  $H_{\mu\nu}^{\text{core}}$  represents the bare-nucleus Hamiltonian matrix accounting for one-electron energies including contributions from kinetic energy plus nuclear-electron attraction.  $J_{\mu\nu}$  denotes matrix elements from classical Coulomb repulsion whereas the third term signifies same for non-classical XC effects. Obviously, this last one constitutes the most difficult and challenging part of whole SCF process.

At this stage, it is noteworthy that basis-set HF method scales as  $N^4$  (total number of two-electron integrals with  $N$  basis functions), while KS calculations do so no worse than  $N^3$ . There have been attempts to develop  $N^2$  or  $N \log N$  scaling algorithms by taking into effect the negligible overlap among basis functions involved. In some earlier LCAO-MO-based KS DFT implementations in GTO bases [81], an *auxiliary* basis set (in addition to the one used for MO expansion) was introduced to fit (by some least square or other technique) some computationally intensive terms to reduce the integral overhead, making it an  $N^3$  process. In one such development [82–84], the electron density and XC potential were expanded in terms of two auxiliary bases  $f_i, g_j$  respectively as,

$$\rho(\mathbf{r}) \approx \tilde{\rho}(\mathbf{r}) = \sum_i a_i f_i(\mathbf{r})$$

$$v_{xc}(\mathbf{r}) \approx \tilde{v}_{xc}(\mathbf{r}) = \sum_j b_j g_j(\mathbf{r}). \quad (16)$$

Here the fitted quantities are identified with tildes while  $\{a_i\}, \{b_j\}$ , the fitting coefficients, are determined by minimization of either a straightforward function of following form,

$$Z = \int [\rho(\mathbf{r}) - \tilde{\rho}(\mathbf{r})]^2 d\mathbf{r}, \quad (17)$$

or Coulomb self-repulsion of residual density. Both are subject to the constraint that normalization of fitted density gives total number of electrons. Originally this technique was first

suggested in the context of STOs [85] and later extended to GTOs [82]. Matrix elements of XC potential (calculated in real-space) were evaluated by some suitable analytical means.

Although this route gained some momentum and was quite successful for many applications, it suffers from some noteworthy difficulties: (i) many distinct fitting techniques with varied flavors (variational or non-variational) produce some inconsistency among various implementations (ii) density and XC fitting constraints differ from method to method (iii) fitting density does not automatically preserve the conservation of total number of electrons (iv) such an approach considerably complicates the analytic derivative theories. At the outset, it may be noted that the main reason for such schemes was primarily due to a lack of efficient method for good-quality multi-center integrals. However, the last few decades has seen emergence of a large number of elegant efficient high-quality quadrature schemes for such integrals offering very accurate results (see, for example, [86], for a lucid review).

Unlike the exchange integrals in HF theory (which are analytically evaluated within a GTO basis), KS theory involves far more challenging non-trivial integrals (due to their complicated algebraic forms). These are not amenable to direct analytic route and resort must be taken to numerical methods.

In this work, the basis functions and MOs are directly built on a real, uniform 3D Cartesian grid simulating a cubic box as,

$$r_i = r_0 + (i - 1)h_r, \quad i = 1, 2, \dots, N_r; \quad \text{for}$$

$$r \in \{x, y, z\}, \quad (18)$$

where  $h_r, N_r$  denote the grid spacing and number of grid points respectively ( $r_0 = -N_r h_r / 2$ ). The classical electrostatic repulsion as well as XC potentials need to be computed on the real grid. For finite systems, possibly the simplest and crudest way to compute  $v_H(\mathbf{r})$  is by direct numerical integration. This, in general, does not perform efficiently and is feasible only for relatively smaller systems. The preferred option is to solve the corresponding Poisson equation. An alternate accurate technique, found to be quite successful in

molecular modeling and used here, involves conventional Fourier convolution method and some variants [66, 67],

$$\begin{aligned} \rho(\mathbf{k}) &= \text{FFT}\{\rho(\mathbf{r})\} \\ v_H(\mathbf{r}) &= \text{FFT}^{-1}\{v_H^c(\mathbf{k})\rho(\mathbf{k})\}. \end{aligned} \quad (19)$$

Here  $\rho(\mathbf{k})$  and  $v_H^c(\mathbf{k})$  represent Fourier integrals of density and Coulomb interaction kernel respectively in the grid. The former is obtained from a discrete Fourier transform of its real-space value by standard FFT quite easily. Evaluation of the latter, however, is a non-trivial task because of the presence of singularity in real space and demands caution. This is overcome by applying a decomposition of the kernel into long- and short-range interactions, reminiscent of the commonly used Ewald summation technique in condensed matter physics,

$$\begin{aligned} v_H^c(\mathbf{r}) &= \frac{\text{erf}(\alpha r)}{r} + \frac{\text{erfc}(\alpha r)}{r} \\ &\equiv v_{H_{\text{long}}}^c(\mathbf{r}) + v_{H_{\text{short}}}^c(\mathbf{r}), \end{aligned} \quad (20)$$

where  $\text{erf}(x)$  and  $\text{erfc}(x)$  correspond to error function and its complement respectively. Short-range Fourier integral can be calculated analytically; the long-range contribution can be obtained directly from FFT of real-space values. There are several other routes as well available for classical repulsion as needed in the large-scale electronic structure within KS DFT framework. More thorough account on this topic can be found in the review [29].

All one-electron contributions of Fock matrix including overlap, kinetic-energy, nuclear-electron attraction as well pseudopotential matrix elements are completely identical to those encountered in HF calculation; these are obtained by standard recursion algorithms [87–89]. Corresponding two-electron matrix elements in real-grid are computed through direct numerical integration in the CCG,

$$\langle \phi_\mu(\mathbf{r}) | v_{HXC}(\mathbf{r}) | \phi_\nu(\mathbf{r}) \rangle = h_x h_y h_z \sum_{\text{grid}} \phi_\mu(\mathbf{r}) v_{HXC}(\mathbf{r}) \phi_\nu(\mathbf{r}). \quad (21)$$

The matrix eigenvalue problem is accurately and efficiently solved using standard LAPACK

routines [90] following usual self-consistent procedure iteratively. The KS eigenfunctions and eigenvalues then give total energies and/or other quantities in the standard manner. Convergence of the solution was monitored through (i) potential (ii) total energies and (iii) eigenvalues. Tolerance of  $10^{-6}$  a.u., was employed for (ii), (iii), while  $10^{-5}$  a.u., for (i).

### III. RESULTS AND DISCUSSION

Table I, at first, displays various quantities for a representative molecule  $\text{Cl}_2$ , in its ground state, at an internuclear distance of 4.20 a.u. Non-relativistic energies as well as other components and total integrated electron density  $N$  are given, for LDA XC potential for different CCG sets, as indicated by grid spacing,  $h$ , and number of grid points,  $N_r$  ( $r \in x, y, z$ ). Several combinations of grid parameters were tested and finally 8 of them are presented here, which is sufficient to illustrate the general important features. Most of these quantities (barring  $E_h, E_x, E_c$ ) are directly comparable with the commonly used versatile GAMESS computer program [77] using same basis function, XC potential and effective core potential. All the LDA calculations referred in this work correspond to the homogeneous electron-gas correlation of Vosko-Wilk-Nusair (VWN) [70]. The Hay-Wadt valence basis set employed here, splits valence orbital into inner and outer components described respectively by two and one primitive Gaussians. Reference values are obtained from two different options, viz., “grid” and “grid-free” DFT. Former uses the default “army” grade with Euler-McLaurin quadratures for radial integration and Gauss-Legendre quadrature for angular integration, while the latter [91, 92] works through a resolution of identity to facilitate evaluation of relevant molecular integration over functionals rather than quadrature grids. As the name implies there is no “grid” in the latter and in a sense, it is quite attractive, as there is no complication that arises from finite grid and associated error. However, there is a price to pay in the form of an *auxiliary* basis set to expand the identity which itself suffers from the same completeness problem. This table illustrates many important points which are explained in detail in [63]. Here we mention some of the most significant observations.

**TABLE I.** Comparison of various energy components of  $\text{Cl}_2$  with reference values at  $R = 4.20$ . CCG and ACG results are given in a.u.

Set	Nr = 32			Nr = 64			Nr = 128			Nr = 256			Ref. [77]
	A	B	C	D	E	F	G	H					
hr	0.3	0.4	0.2	0.3	0.4	0.1	0.2	0.1					
$\langle T \rangle$	11.00750	11.17919	11.18733	11.07195	11.06448	11.18701	11.07244	11.07244	11.07244	11.07244	11.07244	11.07320	
$\langle V_t^{\text{nc}} \rangle$	-83.43381	-83.68501	-83.70054	-83.45722	-83.44290	-83.69988	-83.45810	-83.45810	-83.45810	-83.45810	-83.45810	-83.45964	
$\langle E_h \rangle$	37.94086	36.82427	36.83193	36.58714	36.57918	36.83133	36.58747	36.58747	36.58747	36.58747	36.58747	36.58747	
$\langle E_x \rangle$	-4.86173	-4.86641	-4.86778	-4.84360	-4.84245	-4.86771	-4.84374	-4.84374	-4.84374	-4.84374	-4.84374	-4.84373	
$\langle E_c \rangle$	-0.73575	-0.73521	-0.73530	-0.73374	-0.73366	-0.73530	-0.73374	-0.73374	-0.73374	-0.73374	-0.73374	-0.73374	
$\langle V_t^{\text{ec}} \rangle$	32.34338	31.22265	31.22885	31.00981	31.00306	31.22832	31.01000	31.01000	31.01000	31.01000	31.01000	31.01078	
$\langle E_{\text{nu}} \rangle$	11.66667	11.66667	11.66667	11.66667	11.66667	11.66667	11.66667	11.66667	11.66667	11.66667	11.66667	11.66667	
$\langle V \rangle$	-39.42376	-40.79570	-40.80503	-40.78074	-40.77317	-40.80489	-40.78144	-40.78144	-40.78144	-40.78144	-40.78144	-40.78219	
$\langle E_{\text{el}} \rangle$	-40.08293	-41.28318	-41.28437	-41.37545	-41.37535	-41.28455	-41.37566	-41.37566	-41.37566	-41.37566	-41.37566	-41.37566	
$\langle E \rangle$	-28.41626	-29.61651	-29.61770	-29.70878	-29.70868	-29.61789	-29.70900	-29.70900	-29.70900	-29.70900	-29.70900	-29.70899 <sup>a</sup>	
N	13.89834	13.99939	13.99865	14.00002	14.00003	13.99864	14.00000	14.00000	14.00000	14.00000	13.99999	13.99998	

<sup>a</sup>This is from grid-DFT calculation; corresponding grid-free DFT value is -29.71530 a.u.

First note that Set A shows maximum deviation from reference values for all quantities presumably because the box is not large enough to account for all interactions present in the system. Set B, encompassing a larger box, expectedly offers better results than those in Set A. Interestingly, Sets B,C,F produce very similar results for all the quantities, as they all cover same dimensions; however, results for the last two sets match more closely with each other and differ from Set B, which probably suffers (as reflected in component energies as well as  $N$ ) due to the crudeness of a coarser grid. Sets D,E both produce very good agreement with reference results for all the quantities. In order to test convergence, some extra calculations are done in a much extended grids G,H, which of course, produces very little change. The above discussion leads us to conclude that D,E,G,H are our four best results, while the first two are sufficiently accurate for all practical purposes. For more of these on  $\text{Cl}_2$  and similar discussion on HCl, consult [63].

At this stage, a similar kind of comparison is made for eigenvalues of  $\text{Cl}_2$  and HCl in various grids keeping same basis function, LDA XC potential and pseudopotentials [63]. These are rather less sensitive compared to the quantities

discussed above. For all sets, these either match completely with literature values or show a maximum deviation of only 0.0001-0.0007 a.u. Next, potential energy curves for  $\text{Cl}_2$  and HCl are shown for several sets along with literature results in Fig. I. Total energies are calculated at following ranges of internuclear separation; for  $\text{Cl}_2$ ,  $R = 3.50 - 5.00$  and for HCl,  $R = 1.60 - 3.10$  a.u., both sampled at intervals of 0.10 a.u. It is gratifying that in both occasions CCG results show very close agreement with reference values for entire region of  $R$ . Set D energies for  $\text{Cl}_2$  are quite well (higher from the literature by only 0.0001 a.u.) up to  $R = 4.00$  a.u., and thereafter shows a tendency to deviate gradually (the maximum discrepancy being quite small though; 0.0007 a.u. for  $R = 5.00$  a.u.). Sets G,I for  $\text{Cl}_2$  either match completely with reference values or deviates by a maximum of 0.0001 a.u. Furthermore, we find that our computed energies are always above the reference values, except in two occasions ( $R = 4.00$  and 4.30 for Set G). In HCl, all the sets produce very nice agreement with literature results with Set D performing best. For a more complete discussion see [63].

After demonstrating the dependability and validity of this method, now in Table II, a representative set of 5 atoms and molecules (ordered in ascending

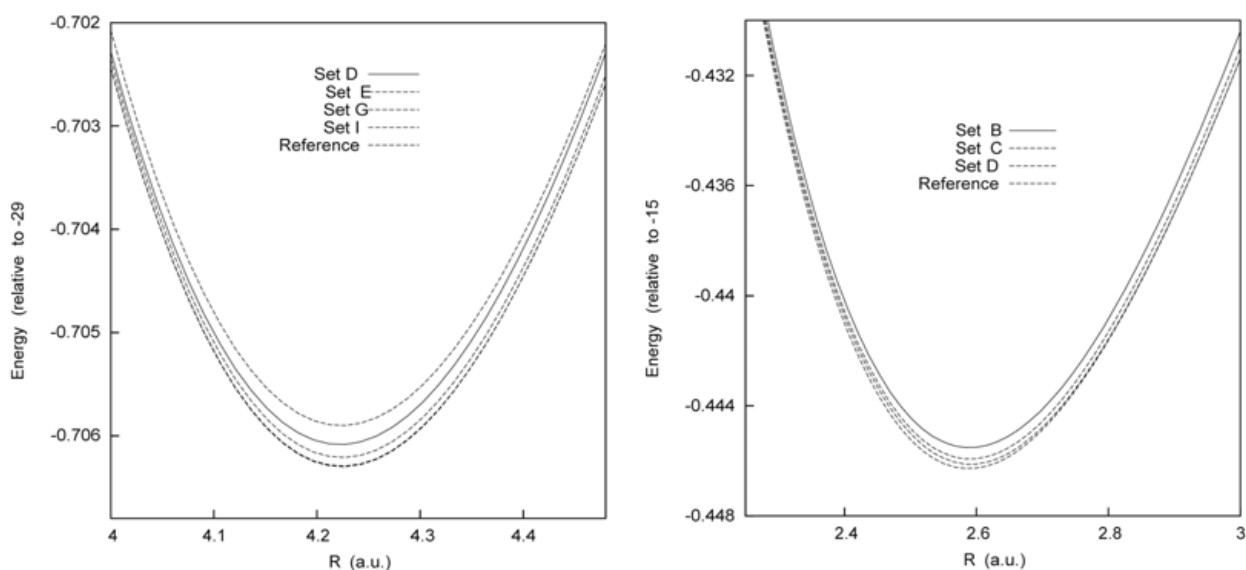


**Fig. 1.** Potential energy curves for  $\text{Cl}_2$  (left panel) and HCl (right panel) in a.u. CCG and ACG results are compared for LDA XC potential.

**TABLE II.** Kinetic energy,  $\langle T \rangle$ , potential energy,  $\langle V \rangle$ , total energy,  $E$ , and  $N$  for selected atoms and molecules (in a.u.) within LDA. CCG and ACG results are compared.

System	$\langle T \rangle$		$-\langle V \rangle$		$-\langle E \rangle$		N	
	CCG	Ref. [77]	CCG	Ref. [77]	CCG	Ref. [77]	CCG	Ref. [77]
NaH	0.56931	0.56912	1.29712	1.29697	0.72781	0.72785	1.99999	2.00005
As	2.07461	2.07354	8.10154	8.10047	6.02693	6.02693	5.00000	4.99999
H <sub>2</sub> S	4.90204	4.90197	16.10707	16.10698	11.20503	11.20501	8.00000	7.99989
Br <sub>2</sub>	8.55754	8.55716	34.74793	34.74755	29.19039	29.19039	14.00000	14.00003
MgCl <sub>2</sub>	11.62114	11.62208	42.34513	42.34621	30.72399	30.72413	16.00004	15.99957

orders of  $N$ ) are presented to assess its performance for a larger set of many-electron systems within the LDA framework. All the quantities, as above were monitored. However, in order to save space, only kinetic, total and potential energy as well as  $N$  are given and compared. In this and all other following tables, experimental geometries are taken from computational chemistry database [93]. These are all done in grid E, which has been found to be quite satisfactory for Cl<sub>2</sub> and HCl. For brevity, we quote only the grid-DFT results for reference, omitting “grid-free” DFT, as we have seen earlier that the two generate results of very similar accuracy. Once again for all of these, excellent agreement is observed; for more details, see [63].

After studying the LDA XC functionals, we now focus into the more important and useful so-called non-local functionals. Well-known problems and discomfitures of LDA functionals for interacting many-electron systems are well documented in numerous communications and it would be necessary to develop more accurate and elegant functionals for future application purposes. A frequently used and extremely successful candidate is the so-called BLYP [71, 72] XC potential having dependence on gradients and Laplacian of density. This is a significant improvement over the LDA case and consequently has found many chemical, physical and biological applications. For practical implementation, however, it is preferable to use an equivalent form of the BLYP functional containing only first derivatives of density, as suggested in [94]. Following [95], this and other gradient-dependent functionals can

be incorporated using a finite-orbital expansion method which helps avoiding the density Hessians. In the end, XC contribution of KS matrix is computed by the following expression,

$$F_{\mu\nu}^{XC\alpha} = \int \left[ \frac{\partial f}{\partial \rho_\alpha} \chi_\mu \chi_\nu + \left( 2 \frac{\partial f}{\partial \gamma_{\alpha\alpha}} \nabla \rho_\alpha + \frac{\partial f}{\partial \gamma_{\alpha\beta}} \nabla \rho_\beta \right) \nabla (\chi_\mu \chi_\nu) \right] d\mathbf{r}, \quad (22)$$

where  $\gamma_{\alpha\alpha} = |\nabla \rho_\alpha|^2$ ,  $\gamma_{\alpha\beta} = \nabla \rho_\alpha \cdot \nabla \rho_\beta$ ,  $\gamma_{\beta\beta} = |\nabla \rho_\beta|^2$ . This is advantageous because  $f$  is a function *only* of local quantities  $\rho_\alpha$ ,  $\rho_\beta$  and their gradients. All non-local functionals in this work are implemented using the Density Functional Repository program [96].

Table III presents a comparison of our CCG energy components for Cl<sub>2</sub> and HCl at  $R = 4.2$  and  $2.4$  a.u., respectively with BLYP functional. A series of calculations along the lines of Table I produced very similar conclusion we reached there for the LDA case. From these numerical experiments, results for a few selected sets are given here, which is sufficient to illustrate the general trend. Again, reference theoretical results correspond to those having same basis function, XC potential and effective core potentials. Both “grid-DFT” results in ACG and “grid-free” DFT results for total energy are reported for comparison. To convince us, some additional reference calculations are performed for a decent number of atoms/molecules in various extended radial and angular grids besides the default grid of  $N_r$ ,  $N_\theta$ ,  $N_\phi = 96, 12, 24$ , namely, (i)  $N_r$ ,  $N_\theta$ ,  $N_\phi = 96, 36, 72$

**TABLE III.** Comparison of BLYP energy components for Cl<sub>2</sub> and HCl in CCG and ACG, in a.u.

Set	Cl <sub>2</sub> (R = 4.2 a.u.)			HCl (R = 2.4 a.u.)		
	A	B	Ref. [77]	A	B	Ref. [77]
N <sub>r</sub>	64	128		64	128	
h <sub>r</sub>	0.3	0.2		0.3	0.2	
⟨T⟩	11.21504	11.21577	11.21570	6.25431	6.25464	6.25458
⟨V <sub>t</sub> <sup>ne</sup> ⟩	-83.72582	-83.72695	-83.72685	-37.29933	-37.29987	-37.29979
⟨E <sub>h</sub> ⟩	36.74464	36.74501		15.86078	15.86103	
⟨E <sub>x</sub> ⟩	-5.29009	-5.29015		-3.01023	-3.01026	
⟨E <sub>c</sub> ⟩	-0.37884	-0.37892		-0.21171	-0.21174	
⟨V <sub>t</sub> <sup>ee</sup> ⟩	31.07572	31.07594	31.07594	12.63884	12.63903	12.63901
⟨E <sub>nu</sub> ⟩	11.66667	11.66667	11.66667	2.91667	2.91667	2.91667
⟨V⟩	-40.98344	-40.98434	-40.98424	-21.74382	-21.74417	-21.74411
⟨E <sub>el</sub> ⟩	-41.43506	-41.43524	-41.43522	-18.40618	-18.40620	-18.40620
⟨E⟩	29.76840	-29.76857	-29.76855 <sup>a</sup>	-15.48951	-15.48953	-15.48953 <sup>b</sup>
N	14.00006	14.00000	13.99998	8.00002	8.00000	8.00000

<sup>a</sup>The *grid-free* DFT value is -29.74755 a.u. [77].

<sup>b</sup>The *grid-free* DFT value is -15.48083 a.u. [77].

(ii) N<sub>r</sub>, N<sub>θ</sub>, N<sub>φ</sub> = 128, 36, 72, with three integers denoting the number of integration points in r, θ, φ directions respectively.

For the set of species chosen, all these grid sets offer results in very close agreement with each other. To summarize, out of 17 species, for 8 of them total energies remain unchanged up to 5th decimal place for all the grids. Very minor variations were observed in remaining cases (largest deviation in total energy occurs for Na<sub>2</sub>Cl<sub>2</sub>, while for all others, it remains below 0.00007). However, as one passes from default grid to (ii), N gradually improves. As evident, CCG results are again in perfect agreement with ACG results, as found for the LDA functional. Obviously Set B produces better results (absolute deviations being 0.00002 and 0.00000 a.u. for Cl<sub>2</sub> and HCl respectively) than Set A, but only marginally. Note that “grid-free” and “grid”-DFT results differ significantly from each other in this

case and for all practical purposes, Set A suffices. Further details can be found in [64].

As in the LDA case, next our calculated BLYP eigenvalues for Cl<sub>2</sub> and HCl (at same R values as in previous tables) are compared in Table IV. Clearly, all the eigenvalues for both molecules are very nicely reproduced, as observed for LDA functionals. Excepting the lone case of 3σ levels (in both cases), where absolute deviation remains only 0.0001 a.u., Sets A,B results show a *complete* matching for *all* orbital energies. In the same vein of our LDA approach earlier, we also investigated total energies and other energy components for a broad range of internuclear distance of Cl<sub>2</sub> (R = 3.5 — 5.0 a.u) and HCl (R = 1.5 — 3.0 a.u.) both with 0.1 a.u. interval for BLYP XC functional. It is very satisfying that for both of them, Sets A,B practically coincide with the reference values for the *entire* range of R. For Cl<sub>2</sub>, maximum absolute deviations of 0.0001 and

**TABLE IV.** Comparison of BLYP negative eigenvalues (in a.u.) of  $\text{Cl}_2$ ,  $\text{HCl}$  with reference values at  $R = 4.2$  and  $2.4$ . CCG and ACG values are given.

MO	$\text{Cl}_2$ ( $R = 4.2$ a.u.)			MO	$\text{HCl}$ ( $R = 2.4$ a.u.)		
	A	B	Ref. [77]		A	B	Ref. [77]
$2u_g$	0.8143	0.8143	0.8143	$2u$	0.7707	0.7707	0.7707
$2u_u$	0.7094	0.7094	0.7094	$3u$	0.4168	0.4167	0.4167
$3u_g$	0.4170	0.4171	0.4171	$1\pi_x$	0.2786	0.2786	0.2786
$1\pi_{xu}$	0.3405	0.3405	0.3405	$1\pi_y$	0.2786	0.2786	0.2786
$1\pi_{yu}$	0.3405	0.3405	0.3405				
$1\pi_{xg}$	0.2778	0.2778	0.2778				
$1\pi_{yg}$	0.2778	0.2778	0.2778				

**TABLE V.** BLYP energy components (in a.u.) and  $N$  for selected atoms, molecules with reference results. CCG results are compared with ACG.

System	$\langle T \rangle$		$-\langle V \rangle$		$-\langle E \rangle$		$N$	
	CCG	Ref. [77]	CCG	Ref. [77]	CCG	Ref. [77]	CCG	Ref. [77]
$\text{Na}_2$	0.14723	0.14723	0.52871	0.52871	0.38148	0.38148	1.99999	2.00000
P	2.38891	2.38890	8.78249	8.78248	6.39358	6.39358	4.99999	4.99999
$\text{NaCl}$	5.83959	5.83957	21.01698	21.01694	15.17739	15.17737	8.00003	7.99999
$\text{PH}_3$	4.18229	4.18224	12.40101	12.40096	8.21871	8.21872	7.99999	7.99999
$\text{H}_2\text{S}_2$	8.88238	8.88240	30.16535	30.16538	21.28297	21.28298	13.99999	13.99999

0.0002 a.u. have been recorded from Sets B,A respectively. For  $\text{HCl}$ , the same remains well below 0.0001 a.u. only. A more thorough discussion is given in [64].

Now Table V compares various energy components (only the kinetic, potential and total energies) for a few selected atoms and molecules with BLYP XC functional (ordered in increasing  $N$  as we descend the table). A smaller grid of  $N_r = 64$ ,  $h_r = 0.4$  was sufficient for atoms, whereas a larger grid  $N_r = 128$ ,  $h_r = 0.3$  was used for molecules. Other energy components are omitted for brevity, as they show very similar agreements with literature values as observed in previous occasions. The overall agreement for these with reference values is excellent. For a set of 5 atoms

and 10 molecules, total energies are found to be identical to those from reference values in 5 occasions; otherwise, the maximum absolute deviation remains below 0.0013%. Results for more atoms and molecules as well as further observations on this can be found in [64].

Finally, Table VI presents the HOMO energies,  $-\epsilon_{\text{HOMO}}$  and atomization energies for selected 7 molecules in LDA and BLYP approximation, at their experimental geometries taken from [93]. From the above discussion, as expected, reference theoretical results are practically identical to those obtained from current CCG work and thus omitted; while available experimental values [97], wherever possible, are quoted appropriately. Experimental atomization energies with asterisks denote 298°K

**TABLE VI.** Comparison of negative HOMO energies,  $-\epsilon_{\text{HOMO}}$  (in a.u.) and atomization energies (kcal/mol) for selected molecules with LDA, LBVWN (LB+VWN) and BLYP XC functionals. Experimental results [97] are also given, wherever possible. An asterisk indicates 298° K values. All others correspond to 0°K.

Molecule	$-\epsilon_{\text{HOMO}}$ (a.u.)				Atomization energy (kcal/mol)		
	LDA	BLYP	LBVWN	Expt. [97]	LDA	BLYP	Expt. [97]
NaBr	0.1818	0.1729	0.3057	0.3050	87.47	78.94	86.8*
SiH <sub>4</sub>	0.3188	0.3156	0.4624	0.4042	339.43	312.02	302.6
S <sub>2</sub>	0.2007	0.2023	0.3443	0.3438	56.75	52.47	100.8
BrCl	0.2623	0.2537	0.4133	0.4079	44.95	25.41	51.5
AlCl <sub>3</sub>	0.3081	0.2976	0.4603	0.4414	278.02	232.88	303.4
P <sub>4</sub>	0.2712	0.2575	0.3964	0.3432	200.77	142.99	285.9
PCl <sub>5</sub>	0.2825	0.2722	0.4397	0.3748	246.22	145.33	303.2

values; otherwise they refer to 0°K. Here ionization energies obtained from a modified Leeuwen-Baerends (LB) exchange potential [98, 99], with LDA correlation is also included for comparison. It may be noted that LDA and GGA XC potentials suffer from incorrect asymptotic long-range behavior; thus although ground-state total energies of atoms, molecules, solids are obtained quite satisfactorily, ionization energies and higher-lying states are described rather poorly. The former is typically off by 30–50% from experimental results. Note that our long-term objective is to investigate the feasibility and applicability of this method for dynamical studies such as laser-atom/molecule interaction through such effects as multi-photon ionization, high-order harmonic generation, photo-ionization, photo-emission, photo-dissociation, etc., within a TDDFT framework. This is a very active, fascinating and challenging area of research from both experimental and theoretical point of view. These processes offer a host of important, fundamental physical and chemical phenomena occurring in such systems and also they have found diverse practical applications (see, for example, [100–105]). For such studies, it is necessary that both ionization energies and higher levels be approximated as accurately as possible, which is unfortunately not satisfied by either LDA or

BLYP functionals. The modified LB potential [98, 99],  $v_{xc\sigma}^{LB\alpha}(\alpha, \beta : \mathbf{r})$ , containing two empirical parameters, seems to be a very good choice in this case and as such, given by,

$$v_{xc\sigma}^{LB\alpha}(\alpha, \beta : \mathbf{r}) = \alpha v_{xc\sigma}^{LDA}(\mathbf{r}) + v_{xc\sigma}^{LDA}(\mathbf{r}) + \frac{\beta x_{\sigma}^2(\mathbf{r}) \rho_{\sigma}^{1/3}(\mathbf{r})}{1 + 3\beta x_{\sigma}(\mathbf{r}) \ln \left\{ x_{\sigma}(\mathbf{r}) + [x_{\sigma}^2(\mathbf{r}) + 1]^{1/2} \right\}}. \quad (23)$$

Here  $\sigma$  signifies up/down spins while the last term containing gradient correction is reminiscent of the exchange functional of [71].  $x_{\sigma}(\mathbf{r}) = |\nabla \rho_{\sigma}(\mathbf{r})| [\rho_{\sigma}(\mathbf{r})]^{-4/3}$  is a dimensionless quantity,  $\alpha = 1.19$ ,  $\beta = 0.01$ . In this approximation of exchange, asymptotic long-range property is satisfied properly, i.e.,  $v_{xc\sigma}^{LB\alpha} \rightarrow -1/r$ ,  $r \rightarrow \infty$ .

Ionization energies obtained from LBVWN (LB exchange+VWN correlation), reported in Column 4, demonstrates its superiority over both LDA and BLYP functionals quite convincingly. LDA values are consistently lower than the corresponding BLYP values while LBVWN energies are lower and more closer to experimental values than both of these. Now calculated atomization energies in columns 6,7 show significant deviations from experimental results. In several occasions,

surprisingly LDA atomization energies are better than their BLYP counterparts. However, this should not be used to conclude the superiority of former over the latter, because there may be some cancellation of errors and also other factors such as more accurate basis functions, core potentials, etc., should be taken in to consideration. Such deviations are not uncommon in DFT, though. Even very elaborate extended basis set all-electron calculations on several molecules show very large errors in a recent work [106]. However this is an on-going activity and does not directly interfere with the main objective of this work.

#### IV. CONCLUDING REMARKS

We presented an alternate route for atomic/molecular calculation using CCG, within the framework of GTO-based LCAO-MO approach to DFT. Although several attempts in real-space are known which use CCG, however, to my knowledge, this is the first time such studies are made in a basis-set approach, *fully* in CCG. Accuracy and reliability of our method is illustrated for a cross-section of atoms/molecules through a number of quantities such as energy components, potential energy curve, atomization energy, ionization potential, eigenvalue, etc. For a large number of species, these results virtually coincide with those obtained from other grid-based or grid-free DFT methods available. The success of this approach lies in an accurate and efficient treatment of the Hartree potential, computed by a Fourier convolution technique by partitioning the interaction in to long-range and short-range components. No auxiliary basis set is invoked in to the picture. Detailed comparisons have been made which shows that the present results are variationally bounded.

#### V. ACKNOWLEDGMENTS

I thank professors D. Neuhauser, S. I. Chu, E. Proynov for useful discussions. I thank the Editor for kind invitation.

#### REFERENCES

1. Parr, R. G. and Yang, W. 1989, Density Functional Theory of Atoms and Molecules, Oxford university Press, New York.
2. Jones, R. O., and Gunnarsson, O. 1989, Rev. Mod. Phys., 61, 689.
3. Dreizler, R. M., and Gross, E. K. U. (Eds.). 1990, Density Functional Theory: An Approach to the Quantum Many-Body Problem, Springer-Verlag, Berlin.
4. Chong, D. P. (Eds). 1995, Recent Advances in Density Functional Methods, World Scientific, Singapore.
5. Seminario, J. M. (Eds.). 1996, Recent Developments and Applications of modern DFT, Elsevier, Amsterdam.
6. Joulbert, D. (Eds.). 1998, Density Functionals: Theory and Applications, Springer, Berlin.
7. Dobson, J. F., Vignale, G., and Das, M. P. (Eds.). 1998, Density Functional Theory: Recent Progress and New Directions. Plenum, New York.
8. Nagy, A. 1998, Phys. Rep., 1, 298.
9. Kohn, W. 1999, Rev. Mod. Phys., 71, 1253.
10. Koch, W. and Holthausen, M. C. 2001, A Chemist's guide to Density Functional Theory, JohnWiley, New York.
11. Parr, R. G., and Sen, K. D. 2002, Reviews of Modern Quantum Chemistry: A Celebration of the Contributions of Robert G. Parr, World Scientific, Singapore.
12. Fiolhais, C., Nogueira, F., and Marques, M. 2003, A Primer in Density Functional Theory, Springer, Berlin.
13. Gidopoulos, N. I. and Wilson, S. 2003, The Fundamentals of Electron Density, Density Matrix and Density Functional Theory in Atoms, Molecules and the Solid State, Springer, Berlin.
14. Martin, R. M. 2004, Electronic Structure: Basic Theory and Practical Methods. Cambridge University Press, Cambridge.
15. Sholl, D. S. and Steckel, J. A. 2009, Density functional Theory: A Practical Introduction, John- Wiley, Hoboken, NJ.
16. Thomas, L. H. 1927, Proc. Camb Phil. Soc., 23, 542.
17. Fermi, E. 1927, Rend. Accad. Lincei, 6, 602.
18. Dirac, P. A. M. 1930, Proc. Camb. Phil. Soc., 26, 376.
19. Hohenberg, P. and Kohn. W. 1964, Phys. Rev. B, 136, 864.

20. Kohn, W. and Sham, L. J. 1965, *Phys. Rev.*, 140, A1133.
21. Laaksonen, L., Sundholm, D., and Pyykko, P. 1985, *Int. J. Quant. Chem.*, 27, 601.
22. Becke, A. D. 1989, *Int. J. Quant. Chem.*, 23, 599.
23. White, S. R., Wilkins, J. W., and Teter, M. P. 1989, *Phys. Rev. B*, 39, 5819.
24. Tsuchida, E. and Tsukada, M. 1995, *Phys. Rev. B*, 52, 5573.
25. Beck, T. L., Iyer, K. A., and Merrick, M. P. 1997, *Int. J. Quant. Chem.*, 61, 341.
26. Hernández, E., Gillan, M. J., and Goringe, C. M. 1997, *Phys. Rev. B*, 55, 13485.
27. Modine, N. A., Zumbach, G., and Kaxiras, E. 1995, *Phys. Rev. B*, 55, 10289.
28. Kim, Y.-H., Staedele, M., and Martin, R. M. 1999, *Phys. Rev. A*, 60, 3633.
29. Beck, T. L. 2000, *Rev. Mod. Phys.*, 72, 1041.
30. Chelikowsky, J. R., Saad, Y., Ogut, S., Vasiliev, I., and Stathopoulos, A. 2000, *Phys. Status Solidi B*, 217, 173.
31. Lee, I.-H., Kim, Y.-H., and Martin, R. M. 2000, *Phys. Rev. B*, 61, 4397.
32. Wang, J. and Beck, T. L. 2000, *J. Chem. Phys.*, 112, 9223.
33. Kronik, L., Makmal, A., Tiago, M. L., Alemany, M. M. G., Jain, M., Huang, X., Saad, Y., and Chelikowsky, J. R. 2006, *Phys. Status Solidi B*, 243, 1063.
34. Chelikowsky, J. R., Troullier, R. N., and Saad, Y. 1994, *Phys. Rev. Lett.*, 72, 1240.
35. Chelikowsky, J. R., Troullier, R. N., Wu, K., and Saad, Y. 1994, *Phys. Rev. B*, 50, 11355.
36. Briggs, E. L., Sullivan, D. J., and Bernholc, J. 1995, *Phys. Rev. B*, 52, R5471.
37. Briggs, E. L., Sullivan, D. J., and Bernholc, J. 1996, *Phys. Rev. B*, 54, 14375.
38. Gygi, F. and Galli, G. 1995, *Phys. Rev. B*, 52, R2229.
39. Lippert, G., Hutter, J., and Parinello, M. 1999, *Theor. Chem. Acc.*, 103, 124.
40. Krack, M. and Parinello, M. 2000, *Phys. Chem. Chem. Phys.*, 2, 2105.
41. Becke, A. D. 1988, *J. Chem. Phys.*, 88, 2547.
42. Gill, P. M. W., Johnson, B. G., and Pople, J. A. 1993, *Chem. Phys. Lett.*, 209, 506.
43. Murray, C. W., Handy, N. C., and G. J. Laming. 1993, *Mol. Phys.*, 78, 997.
44. Treutler, O. and Ahlrichs, R. 1995, *J. Chem. Phys.*, 102, 346.
45. Mura, M. M. and Knowles, P. J. 1996, *J. Chem. Phys.*, 104, 9898.
46. Krack, M. and Köster, A. M. 1998, *J. Chem. Phys.*, 108, 3226.
47. Lindh, R., Malmqvist, P.-A., and Gagliardi, L. 2001, *Theor. Chem. Acc.*, 106, 178.
48. Gill, P. M. W. and Chien, S. H. 2003, *J. Comput. Chem.*, 27, 730.
49. Chien, S. H., and Gill, P. M. W. 2006, *J. Comput. Chem.*, 27, 730.
50. Lebedev, V. I. and Vychisl, Zh. 1975, *Mat. Mat. Fiz.*, 15, 48.
51. Lebedev, V. I. and Vychisl, Zh. 1976, *Mat. Mat. Fiz.*, 16, 293.
52. Lebedev, V. I. and Skorokhodov, A. L. 1992, *Russ. Acad. Sci. Doct. Math.*, 45, 587.
53. Lebedev, V. I. 1994, *Dokl. Akad. Nauk*, 338, 434.
54. Lebedev, V. I. and Laikov, D. N. 1999, *Dokl. Akad. Nauk*, 366, 741.
55. Boerrigter, P. M., te Velde, G. and Baerends, E. J. 1988, *Int. J. Quant. Chem.*, 33, 87.
56. Pederson, M. R. and Jackson, K. A. 1990, *Phys. Rev. B*, 41, 7453.
57. Fusti-Molnar, L. and Kong, J. 2005, *J. Chem. Phys.*, 122, 74108.
58. Brown, S. T., Fusti-Molnar, L., and Kong, J. 2006, *Chem. Phys. Lett.*, 418, 490.
59. Kong, J., Brown, S. T., and Fusti-Molnar, L. 2006, *J. Chem. Phys.*, 124, 094109.
60. Ishikawa, H., Yamamoto, K., Fujima, K., and Iwasawa, M. 1999, *Int. J. Quant. Chem.*, 72, 509.
61. Stratmann, R. E., Scuseria, G. E., and Frisch, M. J. 1996, *Chem. Phys. Lett.*, 257, 213.
62. Yamamoto, K., Fujima, K., and Iwasawa, M. 1997, *J. Chem. Phys.*, 108, 8769.
63. Roy, A. K. 2008, *Int. J. Quant. Chem.*, 108, 837.
64. Roy, A. K. 2008, *Chem. Phys. Lett.*, 461, 142.

- 
65. Roy, A. K. 2009, In Collett, C. T. and Robson, C. D. (Eds.), *Handbook of Computational Chemistry Research*, New York, Nova publishers.
66. Martyna, G. C. and Tuckerman, M. E. 1999, *J. Chem. Phys.*, 110, 2810.
67. Minarray, P., Tuckerman, M. E., Pihakari, K. A., and Martyna, G. J. 2002, *J. Chem. Phys.*, 116, 5351.
68. Wadt, W. R. and Hay, P. J. 1985, *J. Chem. Phys.*, 82, 284.
69. Hay, P. J. and Wadt, W. R. 1985, *J. Chem. Phys.*, 82, 299.
70. Vosko, S. H., Wilk, L., and Nusair, M. 1980, *Can. J. Phys.*, 58, 1200.
71. Becke, A. D. 1988, *Phys. Rev. A*, 38, 3098.
72. Lee, C., Yang, W., and Parr, R. G. 1988, *Phys. Rev. B*, 37, 785.
73. Cramer, C. J. 2004, *Essentials of Computational Chemistry: Theories and Models*. John Wiley, New York.
74. Filatov, M. and Thiel, W. 1997, *Mol. Phys.*, 91, 847.
75. Filatov, M. and Thiel, W. 1997, *Int. J. Quant. Chem.*, 62, 603.
76. Perdew, J. P., Burke, K., and Ernzerhof, M. 1996, *Phys. Rev. Lett.*, 77, 3865.
77. Schmidt, M. W., Baldridge, K. K., Boatz, J. A., Elbert, S. T., Gordon, M. S., Hensen, J. H., Koseki, S., Matsunaga, N., Nguyen, K. A., Su, S. J., Windus, T. L., Dupuis, M., and Montgomery, J. A. 1993, *J. Comput. Chem.*, 14, 1347.
78. Szabo, A. and Ostlund, N. S. 1996, *Modern Quantum Chemistry*, Dover, New York.
79. Jorgensen, P., Helgaker, T., and Olsen, J. 2000, *Modern Electronic Structure Theory*, John Wiley, New York.
80. Jensen, F. 2007, *Introduction to Computational Chemistry*, John Wiley, New York.
81. Andzelm, J. and Wimmer, E. 1992, *J. Chem. Phys.*, 96, 1280.
82. Sambe, H. and Felton, R. H. 1975, *J. Chem. Phys.*, 62, 1122.
83. Dunlap, B. I., Connolly, J. W. D., and Sabin, J. R. 1979, *J. Chem. Phys.*, 62, 1122.
84. Dunlap, B. I., Connolly, J. W. D., and Sabin, J. R. 1979, *J. Chem. Phys.*, 71, 3396.
85. Baerends, E. J., Ellis, D. E., and Ros, P. 1973, *Chem. Phys.*, 2, 41.
86. Gill, P. M. W. 1994, *Adv. Quant. Chem.*, 25, 141.
87. Obara, S. and Saika, A. 1986, *J. Chem. Phys.*, 84, 3963.
88. McMurchie, L. E. and Davidson, E. R. 1978, *J. Chem. Phys.*, 26, 218.
89. Kahn, L. R., Baybutt, P., and Truhlar, D. G. 1976, *J. Chem. Phys.*, 65, 3826.
90. Anderson, E., Bai, Z., Bischof, C., Blackford, S., Demmel, J., Dongarra, J., Du Croz, J., Greenbaum, A., Hammarling, S., McKenney, A., and Sorensen, D. 1999, *LAPACK Users' Guide (3rd Ed.)*. SIAM, Philadelphia.
91. Zheng, Y. C. and Almlof, J. 1993, *J. Chem. Phys.*, 214, 397.
92. Glaesemann, K. R. and Gordon, M. S. 1998, *J. Chem. Phys.*, 108, 9959.
93. Johnson, R. D. III. (Eds.). 2006, *NIST Computational Chemistry Comparisons and Benchmark Database*, NIST Standard Reference Database, Number, Release 14, NIST, Gaithersburg, MD.
94. Miehlich, B., Savin, A., Stoll, H., and Preuss, H. 1989, *Chem. Phys. Lett.*, 157, 200.
95. Pople, J. A., Gill, P. M. W., and Johnson, B. G. 1992, *Chem. Phys. Lett.*, 199, 557.
96. Quantum Chemistry Group. *Density Functional Repository*, CCLRC Daresbury Laboratory, Daresbury, Cheshire, UK.
97. Afeefy, H. Y., Liebman, J. E. 2005, in Linstrom, P. J., Stein, S. E., and Mallard, W. G. (Eds.), *NIST Chemistry Webbook*, NIST Standard Reference Database, Number 69, NIST, Gaithersburg, MD.
98. van Leeuwen, R. and Baerends, E. J. 1994, *Phys. Rev. A*, 49, 2421.
99. Schipper, P. R. T., Gritsenko, O. V., van Gisbergen, S. J. A., and Baerends, E. J. 2001, *J. Chem. Phys.*, 112, 1344.
100. Brabec, T. and Krausz, F. 2000, *Rev. Mod. Phys.*, 72, 545.

- 
101. Udem, Th., Holzwarth, R., and Hansch, T. W. 2002, *Nature (London)*, 416, 233.
  102. Baltuska, A., Udem, Th., Uiberacker, M., Hentschel, M., Goulielmakis, E., Gohle, Ch., Holzwarth, R., Yakolev, V. S., Scrinzi, A., Hansch, T. W., and Krausz, F. 2003, *Nature (London)*, 421, 611.
  103. Stapelfeldt, H. and Seideman, T. 2003, *Rev. Mod. Phys.*, 75, 543.
  104. Posthumus, J. H. 2004, *Rep. Prog. Phys.*, 67, 623.
  105. Gohle, Ch., Udem, Th., Herrmann, M., Rauschenberger, J., Holzwarth, R., Schuessler, H. A., Krausz, F., and Hansch, T. W. 2005, *Nature (London)*, 436, 234.
  106. Cafiero, M. 2006, *Chem. Phys. Lett.*, 418, 126.